J. Fluid Mech. (1985), *vol.* 160, *pp.* 29–45
Printed in Great Britain

Analysis of chemical effects on reflected-shock flow fields in combustible gas

By YASUNARI TAKANO† AND TERUAKI AKAMATSU
Department of Mechanical Engineering, Kyoto University, Japan

(Received 21 October 1982 and in revised form 10 April 1985)

This paper analyses effects of chemical reactions on reflected-shock flow fields in shock tubes. The method of linearized characteristics is applied to analyse gasdynamic disturbances due to chemical reactions. The analysis treats cases where combustible gas is highly diluted in inert gas, and assumes that flows are one-dimensional and that upstream flows in front of the reflected-shock waves are in the frozen state. The perturbed gasdynamic properties in the reflected-shock flow fields are shown to be expressible mainly in terms of a heat-release function for combustion process. In particular, simple relations are obtained between the heat-release function and the physical properties at the end wall of a shock tube. As numerical examples of the analysis, the present formulation is applied to calculate gasdynamic properties in the reflected-shock region in a H_2–O_2–Ar mixture. Procedures are demonstrated for calculation of the heat-release function by numerically integrating rate equations for chemical species. The analytical results are compared with rigorous solutions obtained numerically by use of a finite-difference method. It is shown that the formulation can afford exact solutions in cases where chemical behaviours are not essentially affected by gasdynamic behaviours. When the induction time of the combustion process is reduced to some extent owing to gasdynamic disturbances, some discrepancies appear between analytical results and rigorous solutions. An estimate is made of the induction-time reduction, and a condition is written down for applicability of the analysis.

1. Introduction

The present paper analyses effects of chemical reactions on reflected-shock flow fields in a shock tube. An incident shock wave is produced in the shock tube by the bursting of a diaphragm that separates low-pressure driven gas from high-pressure driver gas. It propagates in the driven section and reflects from a rigid endwall as a reflected shock wave. High-temperature uniform flow is generated behind the incident shock wave and a hot stationary gaseous region is obtained behind the reflected shock wave. Ideally, the physical properties are constant over the shocked regions. Because of these advantages, many experimental investigations for chemical kinetics in a high-temperature gaseous medium have been conducted by utilizing the shock-tube technique. When test gas is added to the driven gas, its chemical process under a constant physical condition can be observed in the shocked gas. However, in actual experiments, these advantages are rather limited. The release of chemical energy according to the progress of chemical reactions causes gasdynamic disturbances. Therefore, in shock-tube experiments for chemical kinetics, reactive gas

† Present address: Department of Applied Mathematics and Physics, Tottori University, Japan.

is often diluted in inert gas to avoid the variation of the physical properties due to reactions.

Chemical effects of the shock-tube flow fields have been investigated for real gases and for combustible mixtures mainly by using numerical procedures, such as the method of characteristics and the finite-difference method. Johannesen, Bird & Zienkiewicz (1967) considered shock reflection in vibrational gas. Presley & Hanson (1969) calculated reflected-shock flow fields in dissociative gas. Dain & Hodgson (1975) studied unsteady flow of a vibrational gas ahead of an impulsively started piston. Takano & Akamatsu (1977) simulated the reflection of ionizing shocks. It has been shown that characteristic flow fields are caused in the shocked region corresponding to chemical relaxation of real gas. The chemical process affects gasdynamics through heat extraction due to vibrational, dissociative or ionization processes. On the other hand, combustion reactions influence fluid motion by mean of heat addition. Gilbert & Strehlow (1966) investigated the detonation initiation behind reflected shocks in H_2–O_2–Ar mixture. Oppenheim *et al.* (1974) studied the dynamic effects of an exothermic process in the reflected-shock region. Mogi, Hasegawa & Asaba (1974) treated the ignition of a hydrogen and oxygen mixture by reflected shock waves. Oran, Young & Boris (1978) developed a simulation model for shock and detonation phenomena. Distinct flow fields are shown to be generated in combustible gas by the coupling mechanism between gasdynamics and chemical kinetics.

As for analyses, Spence (1961) analysed the unsteady motion of a shock wave produced by an impulsively started piston in a relaxing gas. By applying the method of linearized characteristics, he derived analytical forms for variations of the shock speed and for distributions of the pressure and the velocity. Buggisch (1970) gave a short report on shock reflection in relaxing gas, which was explained in the review by Becker (1972). They considered situations where chemical behaviours are not affected by gasdynamic disturbances, and they treated fluid motion and chemical processes separately. A coupled mechanism between gasdynamics and chemical kinetics was considered by Clarke (1978), who studied a problem in which an instantaneously started piston produces a shock wave in explosive gas.

From the standpoint of the experimentalist in chemical kinetics, it is important for precise determination of rate coefficients to estimate the deviation of gasdynamic properties from the idealized values due to chemical reactions. For vibrationally relaxing regions behind ultimately stable shock waves, Johannesen (1961) developed a model from the Rayleigh-line method by treating the real gas as an ideal gas with heat transfer. The method can be used to obtain local rates of relaxation processes from experimental records for the physical properties. One of the motivations of the present analysis is to obtain simple formulas for the perturbed physical properties in the chemically reacting regions behind reflected-shock waves.

The present investigation analyses the gasdynamic behaviours due to combustion processes in reflected-shock regions by using the method of linearized characteristics. It treats cases where combustible gas is diluted in inert ideal gas so that the chemical processes are not affected by the gasdynamic disturbances. It is assumed that the gas flow is one-dimensional and the chemical behaviour upstream of the reflected shock waves is frozen. In the present investigation we consider that perturbed flow fields are caused by the heat transfer due to chemical processes, and try to express the gasdynamic disturbances in terms of a heat-release function. Numerical examples in the present analysis are shown for hydrogen and oxygen diluted in argon gas.

It has been observed that detonations are initiated behind the reflected shock waves in a hydrogen and oxygen mixture as a result of the coupling mechanism between

gasdynamics and chemical kinetics. It should be mentioned that the present results are not always applicable to such explosive phenomena, because the analysis treats fluid and chemical processes separately. In order to consider a limit for validity of the analysis, we compare numerical examples of the analytical results with rigorous solutions obtained from a numerical analysis by use of a finite-difference method. We consider a condition for applicability of the analysis.

2. Basic equations and shock relations

In the present analysis, we treat gasdynamic phenomena due to chemical reactions initiated by shock-heating. As the wave motions proceed much faster than the transport processes, transport effects are ignored here.

The conservation equations for time-dependent one-dimensional reactive gaseous mixtures are (Clarke 1977; Abouseif & Toong 1981)

$$\frac{\partial \boldsymbol{U}}{\partial t}+\frac{\partial \boldsymbol{F}}{\partial x}=0, \tag{1}$$

$$\boldsymbol{U}=\begin{bmatrix}\rho\\ \rho u\\ \rho(e+\frac{1}{2}u^2)\end{bmatrix}, \quad \boldsymbol{F}=\begin{bmatrix}\rho u\\ \rho u^2+p\\ \rho u(e+p/\rho+\frac{1}{2}u^2)\end{bmatrix}, \tag{2a,b}$$

$$\frac{\partial \rho_s}{\partial t}+\frac{\partial(\rho_s u)}{\partial x}=M_s w_s, \quad s=1,\ldots,n, \tag{3}$$

where ρ, u, e and p are respectively the density, velocity, internal energy and pressure of the mixture. The subscript s denotes chemical species in the mixture with n components. M_s and w_s are respectively the molecular weight and mole production rate of the sth species. In the present study the coordinates x and t are respectively the distance from the shock-tube endwall and the time after shock reflection. The density, pressure and enthalpy $h=e+p/\rho$ of the mixture can be written as

$$\rho=\sum_{s=1}^{n}\rho_s, \quad p=\sum_{s=1}^{n}p_s, \quad h=\sum_{s=1}^{n}c_s h_s, \tag{4a,b,c}$$

where c_s $(=\rho_s/\rho)$ is the mass fraction and h_s is the enthalpy for the sth species:

$$h_s=\int_0^T C_{ps}\,\mathrm{d}T+h_s^0. \tag{5}$$

Here T is the temperature, and C_{ps} and h_s^0 are respectively the specific heat and the energy of formation of the sth species. The molecular weight, specific heat and specific-heat ratio for the mixture are defined respectively as

$$M_w=\left(\sum_{s=1}^{n}\frac{c_s}{M_s}\right)^{-1}, \quad C_p=\sum_{s=1}^{n}c_s C_{ps}, \quad \gamma=\frac{C_p}{C_p-R/M_w}, \tag{6a,b,c}$$

where R is the universal gas constant. The thermodynamic equation is written as

$$p=\rho RT/M_w. \tag{7}$$

In addition, the frozen acoustic speed is defined as

$$a\equiv(\gamma p/\rho)^{\frac{1}{2}}. \tag{8}$$

Then the following equations are obtained from (1) and (3):

$$\frac{\partial \boldsymbol{V}}{\partial t}+\boldsymbol{A}\frac{\partial \boldsymbol{V}}{\partial x}=\boldsymbol{B}, \tag{9}$$

where
$$V=\begin{bmatrix}\rho\\u\\p\end{bmatrix},\quad A=\begin{bmatrix}u & \rho & 0\\0 & u & 1/\rho\\0 & \gamma p & u\end{bmatrix},\quad B=\begin{bmatrix}0\\0\\q\end{bmatrix}, \tag{10a,b,c}$$

and
$$\frac{\partial\sigma_s}{\partial t}+u\frac{\partial\sigma_s}{\partial x}=\frac{w_s}{\rho},\quad s=1,\ldots,n, \tag{11}$$

where
$$q=(\gamma-1)\sum_{s=1}^{n}(C_pTM_w-h_sM_s)w_s. \tag{12}$$

Here σ_s $(=c_s/M_s)$ represents the number of moles of the sth species per unit mass of mixture. The mole production rate for the sth species can be written as

$$w_s=\sum_{r=1}^{m}\omega_{sr}, \tag{13}$$

where
$$\omega_{sr}=(\nu'_{sr}-\nu_{sr})X_r(\sigma_1,\ldots,\sigma_n;T,\rho). \tag{14}$$

Here the subscript r denotes elementary reactions, ν'_{sr} and ν_{sr} are the forward and the reverse stoichiometric coefficients of the sth species for the rth reaction, and X_r is the reaction conversion rate for the rth reaction, which will be worked out in §4.

As the endwall of a shock tube is impermeable, the boundary condition is given as

$$u=0\quad\text{at } x=0. \tag{15}$$

At the reflected shock front, the following relation holds in the coordinate system fixed to the shock tube:

$$u_R[U]=[F], \tag{16}$$

where u_R is the speed of the reflected-shock wave, and the square bracket indicates the jump of the physical properties across the shock front. This relation was derived by Lax (1954) from the mathematical theory of nonlinear hyperbolic systems, and also can be deduced from the Rankine–Hugoniot relations.

3. Expansion of basic equations

In the present investigation we consider a situation where combustible gas is diluted in inert ideal gas. Therefore we introduce the following expansions by taking the concentration for reactant as the parameter, ϵ:

$$\rho(x,t)=\rho_i\{1+\epsilon\tilde{\rho}(x',t')+O(\epsilon^2)\},\quad u(x,t)=a_i\{\epsilon\tilde{u}(x',t')+O(\epsilon^2)\}, \tag{17a,b}$$

$$p(x,t)=\rho a_i^2\left\{\frac{1}{\gamma_i}+\epsilon\tilde{p}(x',t')+O(\epsilon^2)\right\},\quad \sigma_s(x,t)=\frac{\delta_{si}}{M_i}+\epsilon\tilde{\sigma}_s(x',t')+O(\epsilon^2), \tag{17c,d}$$

where
$$t=t_r(\epsilon)t',\quad x=a_i t_r(\epsilon)x'. \tag{17e,f}$$

Here the tilde indicates perturbed properties in a normalized form, and the prime is used to denote dimensionless coordinates. The subscript i means physical properties in the reflected-shock region of the flow in which no combustible gas is added to the inert ideal gas. δ_{si} in (17d) is Kronecker's delta, $t_r(\epsilon)$ is the characteristic time for reactions. Figure 1 shows a schematic (x,t)-diagram for the reflected-shock region in inert gas.

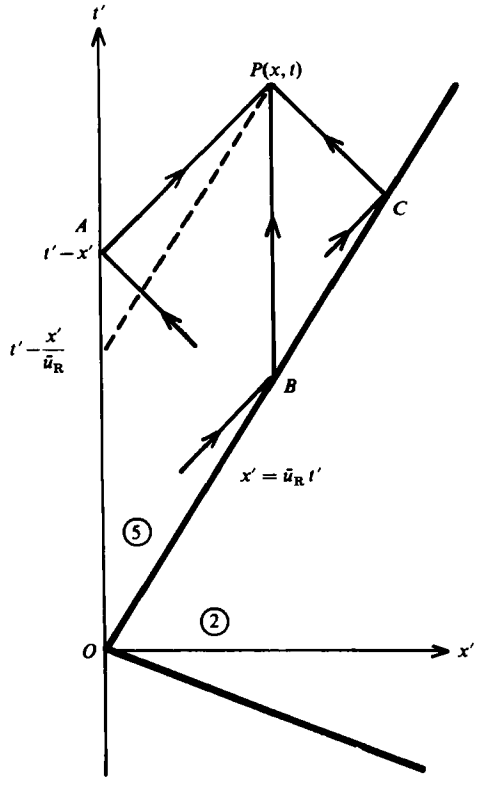

FIGURE 1. Schematic (x, t)-diagram of reflected-shock region.

On substituting this expansion into (8), (13) and (12), these terms can be expanded as power series in ϵ:

$$a = a_1\{1+\epsilon\tilde{a}+O(\epsilon^2)\}, \quad w_s = \frac{\rho_1}{t_r(\epsilon)}\{\epsilon\tilde{w}_s+O(\epsilon^2)\}, \quad q = \frac{\rho_1 a_1^2}{t_r(\epsilon)}\{\epsilon\tilde{q}+O(\epsilon^2)\}, \quad (18a,b,c)$$

where
$$\tilde{q} = M_1 \sum_{s=1}^{n}\left\{1-\frac{h_s(T_1)M_s}{C_{pi}T_1 M_i}\right\}\tilde{w}_s. \quad (18d)$$

The velocity and the position of the reflected shock wave are expressed respectively as

$$u_R(t) = a_1\{\bar{u}_R+\epsilon\tilde{u}_R(t')+O(\epsilon^2)\}, \quad (19a)$$

$$x_R(t) = a_1 t_r(\epsilon)\{\bar{u}_R t'+\epsilon\tilde{x}_R(t')+O(\epsilon^2)\}, \quad (19b)$$

where
$$\tilde{u}_R = d\tilde{x}_R/dt'. \quad (19c)$$

Here $\bar{u}_R$ is the normalized speed of the shock reflection in the inert gas.

3.1. *Linearized equations*

Substituting the expansions (17) into (9) and (11), we obtain for terms of order ϵ,

$$\frac{\partial \tilde{\boldsymbol{V}}}{\partial t}+\bar{\boldsymbol{A}}\frac{\partial \tilde{\boldsymbol{V}}}{\partial x} = \tilde{\boldsymbol{B}}, \quad (20)$$

where

$$\tilde{\boldsymbol{V}} = \begin{bmatrix} \tilde{\rho} \\ \tilde{u} \\ \tilde{p} \end{bmatrix}, \quad \bar{\boldsymbol{A}} = \begin{bmatrix} 0 & 1 & 0 \\ 0 & 0 & 1 \\ 0 & 1 & 0 \end{bmatrix}, \quad \tilde{\boldsymbol{B}} = \begin{bmatrix} 0 \\ 0 \\ \tilde{q} \end{bmatrix}, \tag{21a,b,c}$$

and

$$\frac{\partial \tilde{\sigma}_s}{\partial t} = \tilde{w}_s(\tilde{\sigma}_1, \ldots, \tilde{\sigma}_n; T_1, \rho_1), \quad s = 1, \ldots, n. \tag{22}$$

The equations (22) show that chemical behaviour is treated as not coupled with gasdynamic behaviour. This is because the reaction-rate terms depend on the constant temperature T_1 and the constant density ρ_1 of the reflected-shock region in the inert gas. This decoupling between gasdynamics and chemical kinetics simplifies the integration of the rate equations and also leads to a limitation on the validity of the analysis. We consider the limitation afterwards.

As the matrix $\bar{\boldsymbol{A}}$ has eigenvalues 0, 1 and -1, we transform $\tilde{\boldsymbol{V}}$ to the eigenvectors of $\bar{\boldsymbol{A}}$. Namely, we set

$$r = \tilde{p} + \tilde{u}, \quad s = \tilde{p} - \tilde{u}, \quad \phi = \tilde{p} - \tilde{\rho}. \tag{23a,b,c}$$

Then (20) can be written in terms of the eigenvectors as

$$\left(\frac{\partial}{\partial t} + \frac{\partial}{\partial x}\right) r = \tilde{q}, \quad \left(\frac{\partial}{\partial t} - \frac{\partial}{\partial x}\right) s = \tilde{q}, \quad \frac{\partial \phi}{\partial t} = \tilde{q}. \tag{24a,b,c}$$

The integration of these equations can be performed if the boundary conditions are set. The boundary condition at $x' = 0$ is

$$s = r, \tag{25}$$

because of $u = 0$ at $x = 0$. The other condition for the perturbed flow properties at the shock trajectory $x' = x_R(t')$ is given in §§3.2.

3.2. *Linearized relation for shock wave*

Substituting the expansions (17) and (19a) into the shock relation (16), and equating coefficients of equal powers of ϵ, we obtain the relation of reflected-shock waves in an ideal gas for terms of order 1, and a linearized relation for perturbations of order ϵ. We put the relations

$$\tilde{p} = \tfrac{1}{2}(r+s), \quad \tilde{u} = \tfrac{1}{2}(r-s), \quad \tilde{\rho} = \tfrac{1}{2}(r+s) - \phi, \tag{26a,b,c}$$

(derived from (23)) into the linearized relation for reflected shock waves, and obtain the following boundary conditions:

$$s = Rr, \quad \phi = Lr, \quad \tilde{u}_R = Kr \quad \text{at } x' = x_R(t'), \tag{27a,b,c}$$

where

$$R = \frac{1}{l}\frac{1-m}{1+m}, \tag{28a}$$

$$L = \frac{1}{2}\left(\frac{1-\bar{u}_R}{\bar{u}_R}\right)^2 \left(1 + l\frac{1-m}{1+m}\right), \tag{28b}$$

$$K = \frac{1 + \frac{1}{2}(\gamma_1 - 1)\,\bar{u}_R^2}{(1+\bar{u}_r)\,\bar{u}_R(1+m)}, \tag{28c}$$

and

$$l = \frac{1+\bar{u}_R}{1-\bar{u}_R}, \quad m = 2\frac{\gamma_1 - 1}{\gamma_1 + 1}\left\{\bar{u}_R^2 + \frac{3-\gamma_1}{2(\gamma_1 - 1)}\right\}\frac{1}{\bar{u}_R}. \tag{28d,e}$$

M_S	M_2	$\bar{u}_R$	m	l	R	L	K
1	0	1	1	∞	0	0	0.33
2	0.78	0.67	1.08	5.1	−0.007	0.09	0.49
3	1.04	0.62	1.12	4.3	−0.013	0.14	0.53
4	1.16	0.60	1.13	4.0	−0.015	0.16	0.55
∞	1.34	0.58	1.15	3.7	−0.019	0.20	0.57

TABLE 1. Coefficients and parameters for reflected shock waves ($\gamma_1 = \frac{5}{3}$)

In deriving the above coefficients, it has been assumed that the ratio of specific heats is constant across reflected shock waves in inert ideal gas.

In the limit $\bar{u}_R \to 1$, which corresponds to cases of extremely weak shocks, we observe that $m \to 1$, and consequently R and $L \to 0$ while $K \to \frac{1}{8}(\gamma_1 + 1)$. Behind the incident shock waves, Mach numbers of flows do not rise above the ultimate value of $\{2/\gamma_1(\gamma_1 - 1)\}^{\frac{1}{2}}$. Therefore reflected shock waves in monatomic gas can always be treated as weak or moderate shock waves. Values of coefficients and parameters for reflected-shock waves in monatomic gas with $\gamma_1 = \frac{5}{3}$ are listed in table 1, where M_S is the incident-shock Mach number and M_2 is the Mach number of flows behind incident shock waves. For cases of monatomic gas, the parameter m reduces to $\frac{1}{2}(\bar{u}_R + 1/\bar{u}_R)$. The formulations of the analyses will be simplified by the fact that absolute values of the parameter R are always very small.

3.3. *Integration of linearized equations*

In the present formulation, the boundary conditions at the shock trajectory are applied on $x' = \bar{u}_R t'$ instead of $x' = x_R(t')$. This approximation makes the integration of (22) and (24) straightforward and also causes errors $O(\epsilon \tilde{x}_R)$ for the perturbed terms. Then the expansions (17) are valid as long as $\tilde{x}_R$ remains $O(1)$. However, the shock speed varies from the frozen speed of the shock reflection to a speed ultimately attained after interactions between the reflected shock wave and perturbing waves due to chemical reactions. The deviation of the actual shock trajectory from the frozen one increases with time elapsed after the shock reflection. We will estimate the deviation later.

It has been assumed that the upstream medium in front of the reflected shock front is in a chemically frozen state. Then $\tilde{\sigma}_s$ remains constant along $x' = \bar{u}_R t'$. Therefore we obtain from (22)

$$\tilde{\sigma}_s(x', t') = C_s\left(t' - \frac{x'}{\bar{u}_R}\right), \quad \frac{\mathrm{d}C_s}{\mathrm{d}t'} = \tilde{w}_s(C_1, \ldots, C_n; T_1, \rho_1). \tag{29a, b}$$

The chemical behaviour at order ϵ is shown to proceed coherently in the mixture entering the reflected-shock front. It can also be shown that $\tilde{q}$, the leading term of the expression (18*c*) for the release rate of chemical energy, is a function of the time elapsed after shock heating. This is because $\tilde{q}$ is expressed in terms of $\tilde{w}_s$, which is a function of $t' - x'/\bar{u}_R$ as shown in (22). By making use of this fact, we evaluate solutions for (24) in the domain ranging from $x' = \bar{u}_R t'$ (reflected shock front) to $x' = 0$ (endwall).

When we define an integral function for $\tilde{q}$ as

$$Q(t') = M_1 \sum_{s=1}^{n} \left\{1 - \frac{h_s(T_1) M_s}{C_{p1} T_1 M_1}\right\} \{C_s(t') - C(0)\}, \tag{30}$$

the solution of (24) with the boundary conditions (25) and (27) is expressed in series of Q as

$$r = -\frac{\bar{u}_R}{1-\bar{u}_R} Q\left(t' - \frac{x'}{\bar{u}_R}\right) + \frac{\bar{u}_R}{1+\bar{u}_R}(1+l) \sum_{n=0}^{\infty} R^n Q\left(\frac{t'-x'}{l^n}\right), \tag{31a}$$

$$s = \frac{\bar{u}_R}{1+\bar{u}_R} Q\left(t' - \frac{x'}{\bar{u}_R}\right) + \frac{\bar{u}_R}{1+\bar{u}_R}(1+l) \sum_{n=1}^{\infty} R^n Q\left(\frac{t'+x'}{l^n}\right), \tag{31b}$$

$$\phi = Q\left(t' - \frac{x'}{\bar{u}_R}\right) + L\frac{\bar{u}_R}{1+\bar{u}_R}(1+l) \sum_{n=0}^{\infty} R^n Q\left(\frac{kx'}{l^n}\right), \tag{31c}$$

where $$k = (1-\bar{u}_R)/\bar{u}_R, \tag{31d}$$

and l is defined by (28d).

3.4. *Representation of the flow properties*

The variations of the perturbed gasdynamic properties, which relate to the solution (31) and (26), can be written as

$$\tilde{\rho}(x',t') = \frac{\bar{u}_R}{1-\bar{u}_R^2}\left\{Q(t'-x') - \frac{1}{\bar{u}_R} Q\left(t' - \frac{x'}{\bar{u}_R}\right) - 2LQ(kx')\right\} + O(R), \tag{32a}$$

$$\tilde{u}(x',t') = \frac{\bar{u}_R}{1-\bar{u}_R^2}\left\{Q(t'-x') - Q\left(t' - \frac{x'}{\bar{u}_R}\right)\right\} + O(R), \tag{32b}$$

$$\tilde{p}(x',t') = \frac{\bar{u}_R}{1-\bar{u}_R^2}\left\{Q(t'-x') - \bar{u}_R Q\left(t' - \frac{x'}{\bar{u}_R}\right)\right\} + O(R). \tag{32c}$$

In addition, the variation of the acoustic speed is given as

$$\tilde{a}(x',t') = \tfrac{1}{2}\{\gamma_1 \tilde{p}(x',t') - \tilde{\rho}(x',t') + \Gamma(t'-x')\}, \tag{33}$$

where $$\Gamma(t') = (\gamma_1 - 1) M_1 \sum_{s=1}^{n} \left(1 - \frac{C_{ps} M_s}{C_{p1} M_1}\right)\{C_s(t') - C_s(0)\}. \tag{34}$$

Here the function Γ represents the deviation of the specific-heat ratio for the gaseous mixture. The variation of the temperature is written as

$$\tilde{T}(x',t') = \gamma_1 \tilde{p}(x',t') - \tilde{\rho}(x',t') - M_1 \sum_{s=1}^{n} C_s\left(t' - \frac{x'}{\bar{u}_R}\right). \tag{35}$$

From (27c) and (31a) we obtain the perturbation of reflected-shock velocity as

$$\tilde{u}_R = \frac{2K\bar{u}_R}{1-\bar{u}_R^2} Q((1-\bar{u}_R)t') + O(R). \tag{36}$$

The values of the physical properties at the endwall, which interest experimentalists employing the reflected-shock technique for studies of chemical kinetics, can be obtained by putting $x' = 0$ into (32) and (35):

$$\tilde{p}_w(t') = \frac{\bar{u}_R}{1+\bar{u}_R} Q(t') + O(R), \tag{37a}$$

$$\tilde{\rho}_w(t') = -\frac{1}{1+\bar{u}_R} Q(t') + O(R), \tag{37b}$$

$$\tilde{T}_w(t') = \frac{\gamma_1 \bar{u}_R + 1}{1+\bar{u}_R} Q(t') - M_1 \sum_{s=1}^{n} \{C_s(t') - C(0)\} + O(R). \tag{37c}$$

By using these relations, we will be able to determine experimentally the heat-release function of the combustion process from measurement of the endwall history of the pressure or the density. Also, the deviation of the temperature from the idealized value due to chemical reactions can be estimated by measuring the pressure at the endwall of a shock tube.

It should be mentioned that the formulas (32) are not applicable to the asymptotic reflected-shock flow fields because the trajectory of reflected shock waves is gradually displaced from the linearized one where the boundary condition (27) for shock waves is applied. From (19*c*) and (36), the perturbation of the shock trajectory can be estimated as

$$\tilde{x}_{\mathrm{R}}(t') = \frac{2K\bar{u}_{\mathrm{R}}}{(1+\bar{u}_{\mathrm{R}})(1-\bar{u}_{\mathrm{R}})^2}\,\bar{Q}((1-\bar{u}_{\mathrm{R}})\,t'), \tag{38}$$

where

$$\bar{Q}(t') = \int_0^{t'} Q(t)\,\mathrm{d}t. \tag{39}$$

As $\bar{Q}$ increases with time, errors are introduced into the descriptions for the properties with time.

Several techniques are established to overcome such secular terms in perturbation analyses for inert gasdynamics, as reviewed by Kluwick (1981). It is worthwhile applying these methods to reactive gasdynamics. In the present analysis we do not apply them in the formulation, but leave the coordinate variables untouched. As will be shown in numerical examples of the analysis, the analysis breaks down owing to an interaction between gasdynamics and chemical kinetics *before* its applicability is limited because of the shock-trajectory displacement.

4. Numerical examples

The gasdynamic behaviour of reflected-shock flow fields in H_2–O_2–Ar mixture is calculated as an example for the application of the present formulation. We carried out the computations by using a FACOM M382 Computer in the Data Processing Center at Kyoto University.

4.1. *Chemical kinetics and thermodynamic data*

The combustion systems of a hydrogen and oxygen mixture including inert gas have been extensively studied by employing shock-tube techniques. Getzinger & Schott (1973) wrote a detailed review on shock-tube studies of H_2–O_2 combustion. In the present calculations we consider 13 reactions with 8 species, as listed in table 2. The reaction conversion rates in (14) are now concretely written as

$$X_r = \rho^2 k_r(T)\left\{\sigma_1\sigma_2 - \frac{\sigma_3\sigma_4}{K_r(T)}\right\} \tag{40a}$$

for bimolecular shuffle reactions such as

$$\mathrm{S}_1 + \mathrm{S}_2 = \mathrm{S}_3 + \mathrm{S}_4,$$

and

$$X_r = \rho^3 k_r(T)\,\sigma_i\left\{\sigma_1\sigma_2 - \frac{\sigma_3}{\rho K_r(T)}\right\} \tag{40b}$$

for three-body recombinations such as

$$\mathrm{S}_1 + \mathrm{S}_2 + \mathrm{Ar} = \mathrm{S}_3 + \mathrm{Ar}.$$

For the reaction-coefficient data we use the values given by Jensen & Jones (1978).

		$k_r = A_r T^{n_r} \exp(-T_r/T)$		
r	Reaction	A_r	n_r	T_r
1	$H+O_2=OH+O$	1.54×10^{14}	0	8250
2	$O+H_2=OH+H$	1.80×10^{10}	1	4480
3	$H_2+OH=H_2O+H$	3.78×10^{8}	1.3	1825
4	$O+H_2O=OH+OH$	5.90×10^{13}	0	9120
5	$H+HO_2=OH+OH$	2.40×10^{14}	0	950
6	$OH+HO_2=H_2O+O_2$	3.00×10^{13}	0	0
7	$O+HO_2=OH+O_2$	4.80×10^{13}	0	500
8	$H+HO_2=H_2+O_2$	2.40×10^{13}	0	350
9	$H_2+HO_2=H_2O+OH$	6.00×10^{11}	0	9400
10	$H+O_2+Ar=HO_2+Ar$	1.60×10^{15}	0	−500
11	$H+H+Ar=H_2+Ar$	1.10×10^{18}	−1	0
12	$O+O+Ar=O_2+Ar$	7.25×10^{17}	−1	−200
13	$H+OH+Ar=H_2O+Ar$	3.60×10^{22}	−2	0

T is the temperature in K. Units of rate constants k_r are $cm^3\ mol^{-1}\ s^{-1}$ for $r = 1,\ldots,9$, and $cm^6\ mol^{-2}\ s^{-1}$ for $r = 10,\ldots,13$.

TABLE 2. List of chemical reactions and rate-coefficient data

In the present analysis we have assumed that the medium upstream of the reflected shock waves is in a frozen state. According to Schott & Kinsey (1958), the induction time t_{ind} for stoichiometric H_2–O_2 mixtures diluted with Ar can be approximately expressed as

$$\rho\sigma_{02}\, t_{\mathrm{ind}}\ (\mathrm{mol\ cm^{-3}\ s}) = 2.25\times10^{-8}\exp\left(\frac{9132}{T}\right), \tag{41}$$

over the temperature range $1100 < T < 2600$ K. The ratio between the induction times in the incident-shock region and in the reflected-shock region is over 100, and the assumption is supported in the present numerical examples.

The thermodynamic data are calculated by using the enthalpy coefficients of Gordon & McBride (1976), which give the same values as in the JANAF Thermochemical Tables (Stull & Prophet 1971) within a good precision. In order to calculate the behaviour of the concentrations for the chemical species, we developed a computer program for the numerical integration of the kinetic rate equations (29), referring to the general chemical-kinetics computer program of Bittker & Scullin (1972).

In the present perturbation calculations the mass fraction of oxygen molecules in the initial reactants is chosen as the parameter ϵ. The characteristic time for chemical reactions in (17e,f) is determined by using the coefficient for the first reaction in table 2, which is a rate-controlling reaction in the induction period. Therefore a typical production rate can be written as

$$w_r = k_1(T_{\mathrm{i}})\,\rho_{\mathrm{i}}^2\,\sigma_{02}^2, \quad \sigma_{02} = \epsilon/M_{02},$$

and consequently the characteristic time is

$$t_r(\epsilon) = \frac{\rho_{\mathrm{i}}\sigma_{02}}{w_r} = \left\{\frac{k_1(T_{\mathrm{i}})\,\rho_{\mathrm{i}}\,\epsilon}{M_{02}}\right\}^{-1}. \tag{42}$$

4.2. *Results of calculations*

The results of calculations shown here are carried out for the conditions listed in table 3, where values for several coefficients used in the formulation are also written.

	Unit	Initial state	Incident shock	Reflected shock
Shock speed	km/s	—	0.733	0.436
Density	kg/m^3	0.197	0.502	1.016
Velocity	km/s	0	0.446	0
Pressure	kPa	12	76.3	273.6
Temperature	K	293	730	1295
Acoustic speed	km/s	0.319	0.503	0.670

$M_S = 2.3$, $m = 1.09$, $l = 4.7$, $R = -0.01$, $L = 0.11$

TABLE 3. Physical properties of shock-tube regions in inert gas, and parameters for analytical results

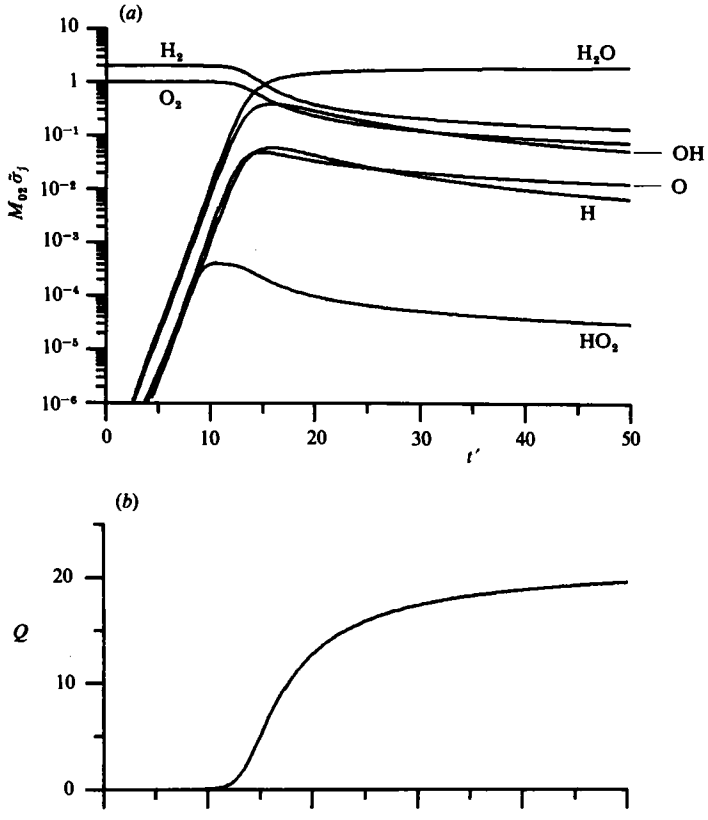

FIGURE 2. (*a*) Variations of concentrations for chemical species in mixture heated by shock wave. (*b*) Heat-release function for combustion process. Simulations are conducted under $T_1 = 1295$ K and $\rho_1 = 1.016$ kg/m^3.

A procedure for evaluation of the formulation is described in the following, referring to the numerical results.

We integrate the kinetic rate equations (29*b*) numerically and obtain the variations of the concentrations $C_s(t')$ for chemical species in the mixture heated by the reflected shock wave. A heat-release function $Q(t')$, defined in (30), can be determined from $C_s(t')$. Figure 2 shows the variation of the concentrations for chemical species and the heat-release function.

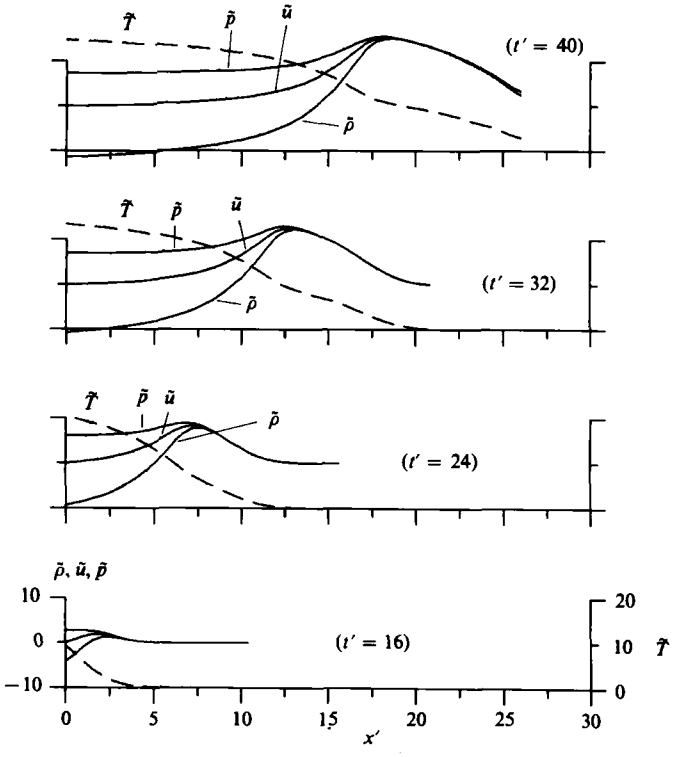

FIGURE 3. Perturbed physical properties in reflected-shock region whose condition is defined in table 3.

Three distinct phases are observed in the combustion process of a stoichiometric hydrogen and oxygen mixture diluted in argon gas, which is instantaneously heated by the reflected shock. In the induction period $0 < t' < 11$ the concentrations of the intermediates, H, O and OH, grow exponentially owing to branching chain reactions (1)–(3) in table 2. Almost no chemical energy is released into the gaseous media in this period. When the intermediates attain certain values in concentration, the formation of H_2O and the consumption of H_2 and O_2 take place rapidly during $11 < t' < 18$, which is called ignition. In the recombination period $t' > 18$ the concentrations of chemical species approach their equilibrium values slowly. The release of chemical energy occurs effectively not only in the ignition phase but also in the recombination phase.

The variations of the physical properties in the perturbed flow field, $\tilde{\rho}$, $\tilde{u}$ and $\tilde{p}$, can be calculated in terms of $Q(t')$, while the variation of the temperature $\tilde{T}$ can be calculated in terms of $Q(t')$ and $C_s(t')$. Figure 3 shows variations of the physical properties in the reflected-shock region, where x' is the distance from the endwall and t' is the time after shock reflection in dimensionless form. For a while after shock reflection, no gasdynamic disturbance is generated behind the reflected shock wave. This is because almost no chemical energy is released in the induction phase. In the induction time, the ignition takes place in the mixture heated by the shock, and exothermic reactions dominate. The heat release begins in the gas adjacent to the endwall, and the pressure and temperature rise in the region with heat addition. Then a compression pulse is caused to propagate away from the endwall. The point where the pressure is maximum in the reflected-shock flow field (for example, it is near

	Unit	Initial state	Incident shock	Reflected shock
Shock speed	km/s	—	0.740	0.436
Density	kg/m^3	0.95	0.500	1.016
Pressure	kPa	12.4†	77.5	277.4
Temperature	K	298	729	1282

† Partial pressures in initial state: Ar, 12 kPa; H_2, 0.27 kPa; O_2, 0.13 kPa.

TABLE 4. Physical properties of shock-tube regions in the frozen state for computational results

$x' = 7.5$ in the graph at $t' = 24$ in figure 3) refers to the start of the ignition phase. It forms a reaction front in the reflected-shock region. We see the perturbed variations of the pressure, the density and the velocity coinciding with each other in front of the reaction front, and understand that an adiabatic compression wave is generated by the pushing of the reaction front. It follows and overtakes the reflected shock wave. In the region behind the reaction front, exothermic reactions dominate. Hence the flow fields are characterized by the release of chemical energy as well as acoustic interactions.

5. Comparisons with rigorous solutions

In explosive gas such as an H_2–O_2 mixture, detonation is observed to develop in the reflected-shock region as a result of severe interaction between fluid motions and chemical processes. When the present analysis is applied to explosive mixture there is a limit of validity because it treats gasdynamics and chemical kinetics separately. (It should be mentioned that interaction between a shock wave and an explosive gas has been investigated by Clarke (1978, 1981).) In order to consider the applicability of the present formulation, we conduct a numerical simulation to obtain exact numerical solutions for (1) and (3) and to compare them with the analytical results. The computational procedure is reported by Takano, Kittaka & Murata (1985), who combine the random-choice scheme for gasdynamics with a simulation code for chemical kinetics to calculate one-dimensional flows of reactive gas consisting of many chemical species with many elementary reactions. The numerical simulation shown here is concerned with gasdynamic phenomena that take place after the reflection of an incident shock wave, at the shock Mach number of 2.28, moving into a stationary mixture of 12 kPa Ar, 0.2667 kPa H_2 and 0.1333 kPa O_2 at room temperature. Table 4 indicates the properties in the initial region, in the region behind the incident shock wave and the region behind the frozen reflected shock wave, where no chemical effect appears yet. The induction time in the reflected-shock region is $t_{\mathrm{ind}} = 0.225$ ms, which is obtained from the simulation. Figure 4 shows pressure profiles in the reflected-shock region, which are plotted with a certain vertical shift at every time interval. From the results of the numerical simulation we obtain perturbed properties due to the chemical reaction, referring to the expansions (17):

$$\tilde{\rho}_{\mathrm{N}}(x', t') = \{\rho_{\mathrm{N}}(x', t') - \rho_{\mathrm{F}}\}/\epsilon, \tag{43a}$$

$$\tilde{u}_{\mathrm{N}}(x', t') = u_{\mathrm{N}}(x', t')/\epsilon, \tag{43b}$$

$$\tilde{p}_{\mathrm{N}}(x', t') = \gamma_{\mathrm{F}}\{p_{\mathrm{N}}(x', t') - p_{\mathrm{F}}\}/\epsilon, \tag{43c}$$

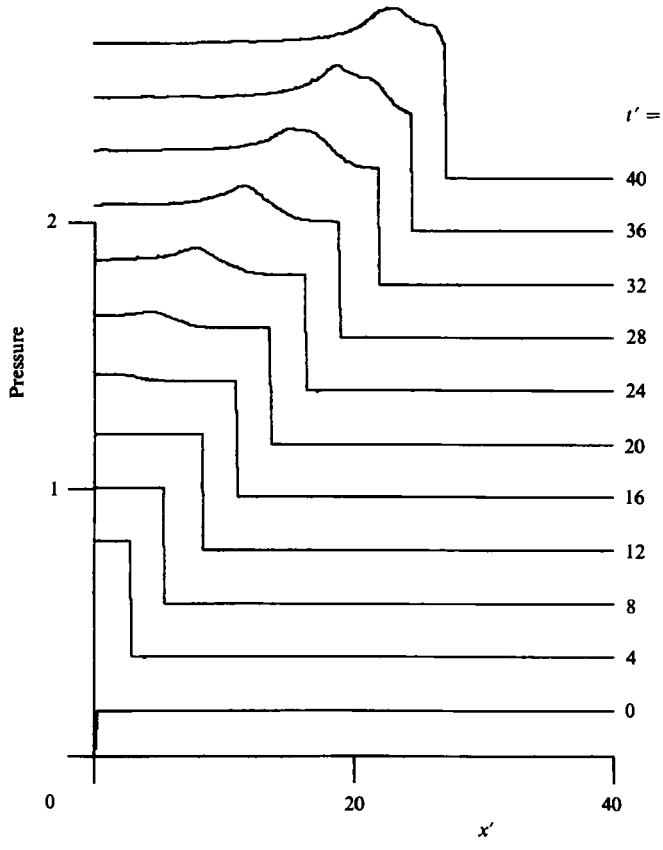

FIGURE 4. Pressure profiles in reflected-shock region whose condition is given in table 4; $t_r = 15.4\ \mu s$, $x_r = a_F t_r = 10.3$ mm.

where subscript N denotes results of the numerical simulation, and subscript F denotes values of the frozen physical properties in the reflected-shock region. The parameter ϵ, which corresponds to the mass fraction of oxygen molecules in the initial state, is 0.0088 for the computational results. Figure 5 shows a comparison between analytical and computational results of the perturbed properties at $t' = 20$. The agreement is excellent between them. Hence it is shown that the present formulation can afford exact solutions of perturbed flow fields due to chemical reactions.

Figure 6 shows a comparison between a computed flow field at $t' = 28$ and an analytically derived one at $t' = 30$. We choose them so that reaction fronts in both results may overlap each other. In the present framework of analysis, the reaction front propagates at the same speed as the reflected shock wave. Therefore the induction distance from the reflected shock wave to the reaction front does not change at all in the analytical results. On the other hand, the induction distance is reduced by about 10 % in the numerical simulation. Also, differences of the properties for both results are estimated to be approximately 20 % in the neighbourhood of the accelerating reaction front. The reduction of induction time is caused by perturbations in the properties, especially the temperature rise, in the induction region between the reflected shock wave and the reaction front. Unless the variation of induction time remains small, the analytical results become questionable.

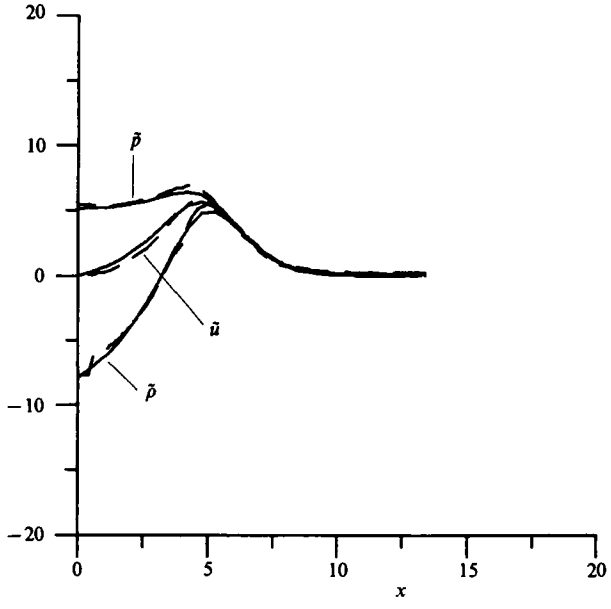

FIGURE 5. Comparisons between analytical results (——) and computational results (– – –) at $t' = 20$.

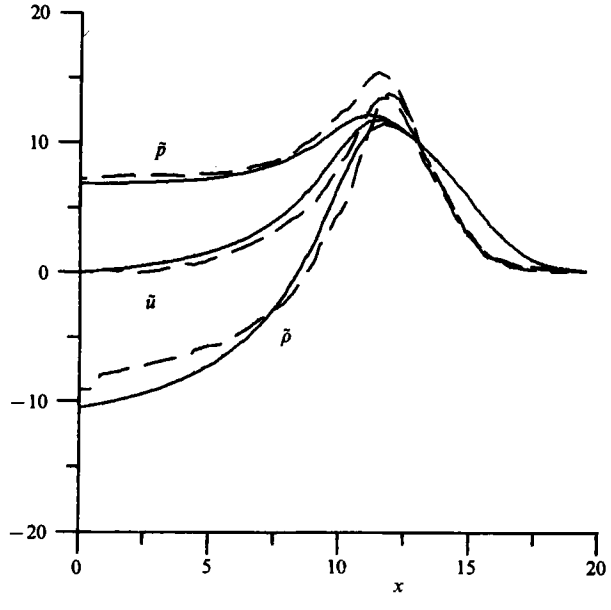

FIGURE 6. Comparisons between analytical and computational results; ——, analytical results at $t' = 30$; – – –, computational results at $t' = 28$.

The reduction of induction time can be estimated from (41) as follows:

$$\frac{\Delta t_{\text{ind}}}{t_{\text{ind}}} = -\beta \frac{\Delta T}{T_1}, \tag{44}$$

when the temperature changes slightly by ΔT on average over the induction region.

Here $\beta = T_A/T_i$ and T_A (= 9132 K for the present example) is the empirical activation temperature. The expression (44) is valid as long as

$$\left|\beta \frac{\Delta T}{T_i}\right| \ll 1. \tag{45}$$

The temperature variation averaged along a particle path in the induction region can be written as

$$\frac{\Delta T}{T_i} = \epsilon \frac{1}{t'_{ind}} \int_{x'/\bar{u}_R}^{t'_{ind}+x'/\bar{u}_R} \bar{T}(x', t)\, dt, \tag{46}$$

where t'_{ind} (= $t_{ind}/t_r(\epsilon)$) is the normalized induction time.

As the heat release essentially does not occur in the induction region, the temperature perturbation can be written approximately as

$$\bar{T}(x', t') \approx (\gamma_i - 1) \frac{\bar{u}_R}{1-\bar{u}_R^2} Q(t'-x') \tag{47}$$

for

$$\frac{x'}{\bar{u}_R} \leqslant t' \leqslant t'_{ind} + \frac{x'}{\bar{u}_R};$$

(44) then reduces to

$$\frac{\Delta t'_{ind}}{t_{ind}} = -\beta\epsilon(\gamma_i - 1) \frac{\bar{u}_R^2}{1-\bar{u}_R^2} \frac{1}{t'_{ind}} \bar{Q}\left(t'_{ind} + \frac{1-\bar{u}_R}{\bar{u}_R} x'\right) \tag{48}$$

for

$$0 \leqslant \frac{1-\bar{u}_R}{\bar{u}_R} x' \leqslant t'_{ind}.$$

Here $\bar{Q}$ (defined in (39)) is the integral function of Q. The limit of the applicability depends on how much error is permitted. If it is considered that 10 % reduction of the induction time is permitted, the condition for validity can be expressed as

$$\frac{\epsilon}{t'_{ind}} \bar{Q}\left(t'_{ind} + \frac{1-\bar{u}_R}{\bar{u}_R} x'\right) < 0.02. \tag{49}$$

This is because $\gamma_i = \frac{5}{3}$, $\beta \approx 7$ and $\bar{u}_R \approx 0.65$.

6. Conclusions

The method of linearized characteristics has been applied to analyse gasdynamic disturbances due to chemical reactions in the reflected-shock regions of shock tubes. The analysis treats cases where combustible gas is diluted in inert gas so that chemical behaviour is not affected by the gasdynamic behaviour. It assumes that flows are one-dimensional and flows upstream of the reflected shock wave are frozen.

The perturbed gasdynamic properties in the reflected-shock flow fields are shown to be expressible mainly in several series terms of a heat-release function for combustion process. Simple relations are obtained between the heat-release function and the physical properties at the endwall of a shock tube.

As numerical examples of the analysis, the present formulation has been applied to calculate gasdynamic properties in the reflected-shock region in a H_2–O_2–Ar mixture. The analytical results have been compared with rigorous solutions, which have been obtained by employing the finite-difference technique. It is shown that the present formulation can afford exact solutions in cases where chemical behaviour is not essentially affected by gasdynamic behaviour. However, it cannot give proper

descriptions for fluid motions when the gasdynamic disturbances reduce the induction time and accelerate the reaction front.

There remain further problems which have not been resolved in the present investigation: an analysis should be performed to include the acceleration effect of the reaction front. Secular terms relating to the shock trajectory should be overcome by applying techniques which are established for nonlinear effects in gasdynamics.

REFERENCES

Abouseif, G. E. & Toong, T. Y. 1981 *J. Fluid Mech.* **103**, 1–22.

Becker, E. 1972 *Ann. Rev. Fluid Mech.* **4**, 155–194.

Bittker, D. A. & Scullin, V. J. 1972 *NASA TN* d-6586.

Buggisch, V. H. 1970 *Z. angew. Math. Mech.* **50**, T168–T170.

Clarke, J. F. 1977 *J. Fluid Mech.* **81**, 257–264.

Clarke, J. F. 1978 *Cranfield Inst. Tech. College of Aeronautics Memo* 7801.

Clarke, J. F. 1981 *Combustion in Reactive Systems; Prog. Astronautics Aeronautics*, **76**, 383–402.

Dain, C. G. & Hodgson, J. P. 1975 *J. Fluid Mech.* **69**, 129–144.

Gilbert, R. B. & Strehlow, R. A. 1966 *AIAA J.* **4**, 1777–1783.

Getzinger, R. W. & Schott, G. L. 1973 *Physical Chemistry of Fast Reactions*, vol. 1 (ed. B. P. Levitt), chap. 2, pp. 81–160. Plenum.

Gordon, S. & McBride, B. J. 1976 *NASA* SP-273.

Kluwick, A. 1981 *Prog. Aerospace Sci.* **19**, 197–313.

Jensen, D. E. & Jones, G. A. 1978 *J. Combust. Flame* **32**, 1–34.

Johannesen, N. H. 1961 *J. Fluid Mech.* **10**, 25–32.

Johannesen, N. H., Bird, G. A. & Zienkiewicz, H. K. 1969 *J. Fluid Mech.* **30**, 51–64.

Lax, P. D. 1954 *Communs Pure Appl. Maths* **7**, 159–193.

Mogi, Y., Hasegawa, K. & Asaba, T. 1974 *Acta Astronautica* **1**, 921–933.

Oppenheim, A. K., Cohen, L. M., Short, J. M., Chen, R. K. & Hom, K. 1974 In *Proc. 15th Symp. (Intl) on Combustion*, pp. 1503–1513. The Combustion Institute.

Oran, E., Young, T. & Boris, J. 1978 In *Proc. 17th Symp. (Intl) on Combustion*, pp. 43–54. The Combustion Institute.

Presley, L. L. & Hanson, R. K. 1969 *AIAA J.* **7**, 2267–2273.

Schott, G. L. & Kinsey, J. L. 1958 *J. Chem. Phys.* **29**, 1177–1182.

Spence, D. A. 1961 *Proc. R. Soc. Lond.* A **262**, 221–234.

Stull, D. A. & Prophet, H. 1971 *JANAF Thermochemical Tables.* NSRDS-NBS37.

Takano, Y. & Akamatsu, T. 1977 *Z. Naturforsch.* **32a**, 986–993.

Takano, Y., Kittaka, S. & Murata, S. 1985 *Trans. JSME* (to appear).